Quaternary Science Reviews 263 (2021) 106993

Contents lists available at ScienceDirect

Quaternary Science Reviews

journal homepage: www.elsevier.com/locate/quascirev

Late Pleistocene paleoecology and phylogeography of woolly rhinoceroses

Alba Rey-Iglesia [a, *], Adrian M. Lister [b], Anthony J. Stuart [c], Hervé Bocherens [d, e], Paul Szpak [f], Eske Willerslev [a], Eline D. Lorenzen [a, **]

[a] GLOBE Institute, University of Copenhagen, 1350, Copenhagen K, Denmark
[b] Earth Sciences Department, Natural History Museum, London, SW7 5BD, UK
[c] Department of Biosciences, Durham University, Durham, DH1 3LE, UK
[d] Department of Geosciences, Tübingen University, 72074, Tübingen, Germany
[e] Senckenberg Centre for Human Evolution and Palaeoenvironment, 72074, Tübingen, Germany
[f] Department of Anthropology, Trent University, Peterborough, Ontario, K9L 0G2, Canada

ARTICLE INFO

Article history:
Received 11 January 2021
Received in revised form
24 April 2021
Accepted 12 May 2021
Available online xxx

Handling Editor: Danielle Schreve

Keywords:
Ancient DNA
Coelodonta antiquitatis
Late pleistocene
Mitochondrial DNA
Paleoecology
Stable isotopes
Woolly rhinoceros

ABSTRACT

The woolly rhinoceros (*Coelodonta antiquitatis*) was a cold-adapted herbivore, widely distributed from western Europe to north-east Siberia during the Late Pleistocene. Previous studies have associated the extinction of the species ~14,000 calendar years before present to climatic and vegetational changes, suggesting the later survival of populations in north-east Siberia may have related to the later persistence of open vegetation in the region. Here, we analyzed carbon ($\delta^{13}C$) and nitrogen ($\delta^{15}N$) stable isotopes and mitochondrial DNA sequences to elucidate the evolutionary ecology of the species. Our dataset comprised 286 woolly rhinoceros isotopic records, including 192 unpublished records, from across the species range, dating from >58,600 to 12,135 ^{14}C years before present (equivalent to 14,040 calendar years ago). Crucially, we present the first 71 isotopic records available to date of the 15,000 years preceding woolly rhinoceros extinction. The data revealed ecological flexibility and geographic variation in woolly rhinoceros stable isotope compositions across time. In north-east Siberia, we detected stability in $\delta^{15}N$ through time, which could reflect long-term environmental stability, and may have enabled the later survival of the species in the region. To further investigate the paleoecology of woolly rhinoceroses, we compared their isotopic compositions with other contemporary herbivores. Our findings suggested isotopic similarities between woolly rhinoceros and both musk ox (*Ovibos moschatus*) and saiga (*Saiga tatarica*), albeit at varying points in time, and possible niche partitioning between woolly rhinoceros and both horse (*Equus* spp.) and woolly mammoth (*Mammuthus primigenius*). To provide phylogeographic context to the isotopic data, we compiled and analyzed the 61 published mitochondrial control region sequences. The genetic data showed a lack of geographic structuring; we found three haplogroups with overlapping distributions, all of which showed a signal of expansion during the Last Glacial Maximum. Furthermore, our genetic findings support the notion that environmental stability in Siberia influenced the paleoecology of woolly rhinoceroses in the region. Our study highlights the utility of combining stable isotopic records with ancient DNA to advance our knowledge of the evolutionary ecology of past populations and extinct species.

1. Introduction

The Late Pleistocene was characterized by large-scale climatic and environmental change (Hubberten et al., 2004). Around 33 thousand years before present (ka BP), a progressive cooling started, which led to the cold and dry environment of the Last Glacial Maximum (LGM; ~28.6–20.5 ka BP) (Kuitems et al., 2019). This was followed by an increase in temperature, which peaked at the start

* Corresponding author.
** Corresponding author.
E-mail addresses: ardelaiglesia@sund.ku.dk (A. Rey-Iglesia), elinelorenzen@sund.ku.dk (E.D. Lorenzen).

https://doi.org/10.1016/j.quascirev.2021.106993

of the Holocene 11.7 ka BP. These pronounced climatic perturbations led to shifts in the geographic distribution of species and in the composition of entire ecosystems.

During the Late Pleistocene, large mammal species, including cave bear (*Ursus spelaeus*), cave lion (*Panthera spelaea*), and woolly rhinoceros (*Coelodonta antiquitatis*) went extinct in northern Eurasia (Pacher and Stuart, 2009; Stuart and Lister 2011, 2012). Other Pleistocene megafauna, including giant deer (*Megaloceros giganteus*) and woolly mammoth (*Mammuthus primigenius*), experienced strong reductions in their distributions during the Late Pleistocene, but only disappeared from the faunal record later, during the Holocene (Stuart et al., 2002; Lister and Stuart, 2019). These different extinction patterns among species have been attributed to the interplay of several drivers, including climatic, anthropogenic, and/or genetic factors (Cooper et al., 2015; Pečnerová et al., 2017).

In the northern hemisphere, Late Pleistocene glacial phases were characterized by the mammoth steppe ecosystem, which comprised a mosaic of steppe-tundra and shrub vegetation, with high nutrient soils that enabled the growth of plants that sustained grazing species (Guthrie 1982, 2001). The mammoth steppe extended from the northern Iberian Peninsula to Canada, and was characterized by a diverse community of large herbivores.

The woolly rhinoceros was one of the iconic inhabitants of this steppe-tundra ecosystem. The species was adapted to cold environments; it was covered with thick and long hair, as documented by mummified remains, but is believed to not have been well adapted to snowfall, due to its massive body on short legs (Boeskorov et al., 2011). Teeth structure and mesowear analysis indicate a grazing diet (Stuart and Lister, 2012; Rivals and Lister, 2016; Stefaniak et al., 2020), which is supported by grass remains recovered between the teeth of some specimens (Guthrie, 1990). Microwear analysis of North Sea woolly rhinoceroses suggests periodical inclusion of woody components in their diet (van Geel et al., 2019). Pollen analysis of stomach contents has primarily identified grasses and sagebrushes (e.g. Boeskorov et al., 2011), and genetic analysis of stomach and gut content supports a diet of primarily grasses, with a contribution of forbs (Willerslev et al., 2014).

Prior to their extinction ~14 thousand calendar years before present (cal kyr BP), woolly rhinoceroses ranged from western Europe to north-east Siberia (Fig. 1). Specimens have not been recovered from certain areas in Europe and north-central Siberia, suggesting the species was absent from these regions (Stuart and Lister, 2012). Despite their presence in the fossil record in far northeastern Siberia, adjacent to the Bering Land Bridge, woolly rhinoceroses did not colonise North America; it has been suggested that the environmental conditions of the Bering Land Bridge and the paleoecology of eastern Beringia (present-day Alaska and Yukon territory) were not adequate for the species (Boeskorov, 2011; Stuart and Lister, 2012).

Despite a progressive eastward contraction in the species' fossil record starting ~35 cal kyr BP (Stuart and Lister, 2012), fossil evidence indicates woolly rhinoceroses were still present in large parts of Eurasia until ~16 cal kyr BP, suggesting an almost synchronous or at least rapid extinction across their range (Lorenzen et al., 2011). Demographic modelling based on genomic data has documented a population increase ~30 cal kyr BP, followed by demographic stability until close to woolly rhinoceros extinction (Lord et al., 2020). From 14.6 cal kyr BP, the range of the species had contracted so that woolly rhinoceroses were found only in the Ural Mountains, southern Siberia, and NE Siberia. The most recent fossil records are ~14 cal kyr BP from NE Siberia; the youngest fossil has been dated to 12,135 ^{14}C years BP or 14,040 cal yr BP (Boeskorov, 2011; Stuart and Lister, 2012).

Climate and vegetational changes have in combination been invoked as the main causative agents of woolly rhinoceros extinction (Lorenzen et al., 2011; Stuart and Lister, 2012; Lord et al., 2020). Environmental shifts included increased ground moisture due to precipitation and snowfall in the Late Glacial Interstadial (14.7−12.9 cal kyr BP) (Sher, 1997), and the spread of shrubs and trees (Stuart and Lister, 2012). These new environmental conditions would have restricted areas of firm ground and open vegetation that are believed to have been the most suitable habitat for woolly rhinoceroses (Stuart and Lister, 2012). The later survival of the woolly rhinoceros in NE Siberia may be linked to the late persistence of open vegetation in the region, compared with the rest of Eurasia (Stuart and Lister, 2012). NE Siberia also played a key role for other Late Pleistocene megafauna species, and the region was the last mainland area of survival of both steppe bison (*Bison priscus*) and woolly mammoth prior to their extinctions (Vartanyan et al., 1993; Kirillova et al., 2015a).

Stable isotope (δ^{13}C and δ^{15}N) analysis of bone and tooth collagen have provided important insights into the diet and paleoecology of Late Pleistocene megafauna, including brown bear (*Ursus arctos*), cave bear, cave lion, giant rhinoceros (also known as Siberian unicorn, *Elasmotherium sibiricum*), musk ox, saiga (*Saiga tatarica*), and woolly mammoth (Iacumin et al., 2000; Szpak et al., 2010; Bocherens et al., 2011; Raghavan et al., 2014; Krajcarz et al., 2016; Jürgensen et al., 2017; Arppe et al., 2019; Kosintsev et al., 2019; Rey-Iglesia et al., 2019). δ^{13}C and δ^{15}N have also been used to investigate the paleoecology and paleodiet of woolly rhinoceroses (Bocherens et al. 1995, 1996, 1997, 2005, 2011, 1996, 2005; Higham et al., 2006; Jacobi et al. 2006, 2007, 2009, 2007; Kirillova et al., 2015b; Yates et al., 2017; Stefaniak et al., 2020). However, in contrast with work on e.g. musk ox, saiga, and woolly mammoth (Szpak et al., 2010; Raghavan et al., 2014; Jürgensen et al., 2017), a range-wide study of woolly rhinoceros paleoecology and paleodiet based on stable isotope data has so far been lacking.

In herbivores, δ^{13}C and δ^{15}N values reflect the isotopic compositions of plants in their diet (DeNiro, 1985; Bocherens, 2003), the composition of which is in turn influenced by climatic and environmental factors (Hartman, 2011; Bonafini et al., 2013). Carbon isotopic compositions in herbivore bone and tooth collagen reflect the photosynthetic pathways and environmental parameters of plants at the base of the food web (Bocherens, 2003). Nitrogen derives from the plant protein the animal digests; dietary choices may lead to differences in δ^{15}N, even at the same trophic level (Bocherens, 2003). Furthermore, environmental factors such as water stress, salinity or grazing pressure, are known to affect plant δ^{15}N values, and changes in vegetation and soil nutrient cycling will therefore be recorded in bone and tooth collagen.

In this study, we analyzed δ^{13}C and δ^{15}N retrieved from woolly rhinoceros remains spanning 45 kyr of evolutionary history. We present 192 new isotopic records from across the species range, dating from >58,600 to 12,135 ^{14}C years before present (equivalent to 14,040 calendar years ago). These include 71 isotopic records from the 15 kyr preceding woolly rhinoceros extinction, which represent the first available stable isotope records from this period. We combined the 192 new records with published δ^{13}C and δ^{15}N data of 94 woolly rhinoceroses, totalling 286 samples, to (i) investigate temporal and spatial changes in woolly rhinoceros diet and ecology; (ii) specifically assess changes in the millennia preceding extinction; and (iii) elucidate the later survival of the species in NE Siberia.

To understand the broader ecological context of our findings, we compared the woolly rhinoceros stable isotope records with comparative data from five other contemporaneous megaherbivore species (horse (*Equus* spp.), musk ox, reindeer (*Rangifer tarandus*), saiga, woolly mammoth).

To elucidate the phylogeographic context of the

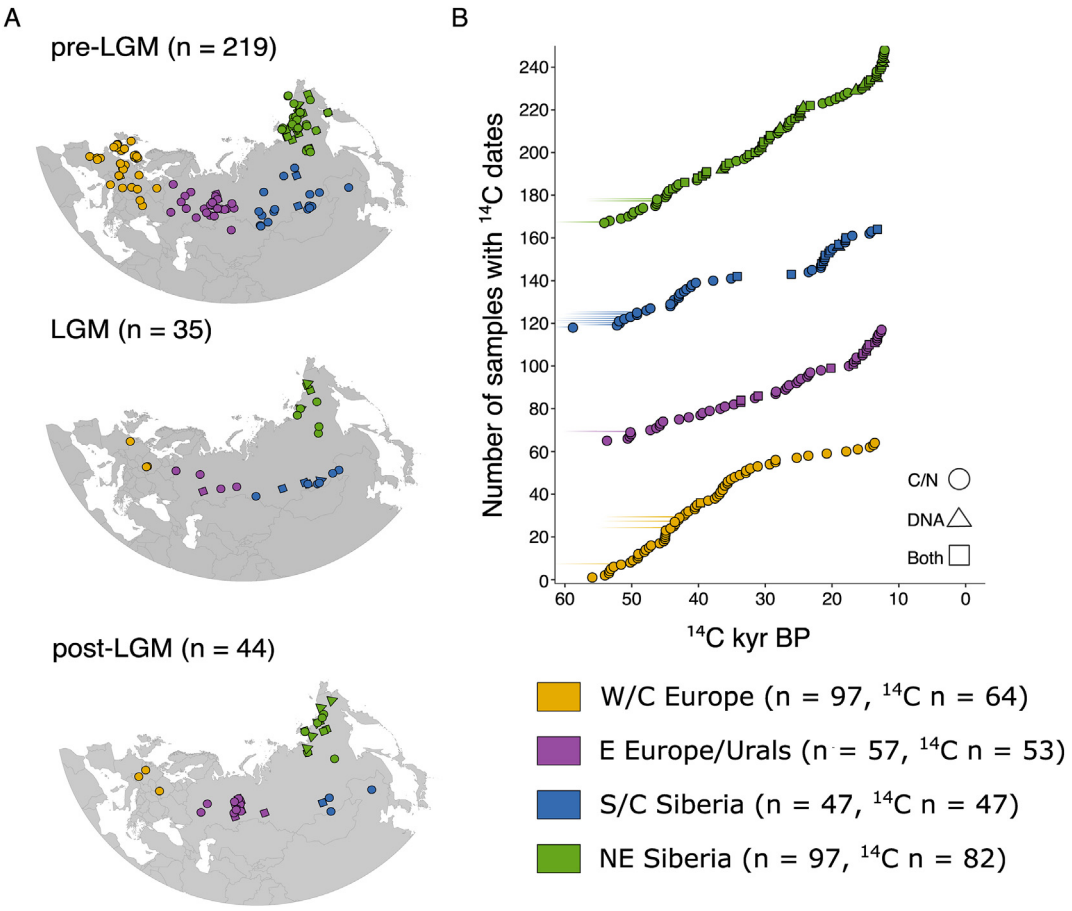

Fig. 1. (A) Map of sample locations of the 298 woolly rhinoceros remains analyzed in this study for stable isotopes and DNA. The samples were split into four geographic regions, indicated by different colours. Shapes represent data type: stable isotopes (circle), DNA (triangle), and both (square). Maps show three time bins: pre-LGM (>24,600 ^{14}C years BP/ 28,660 cal years BP), LGM (24,600–17,000 ^{14}C years BP/28,660–20,520 cal years BP), and post-LGM (<17,000 ^{14}C years BP/< 20,520 cal years BP). (B) Chronology of the ^{14}C radiocarbon dated samples used in this study for each geographic region. Plotted dates represent uncal ^{14}C years BP, extended lines represent infinite dates. Symbol colour and shape represent region and data type, respectively. Sample size (n = all samples, n = ^{14}C dated samples) is indicated for each geographic region. (For interpretation of the references to colour in this figure legend, the reader is referred to the Web version of this article.)

palaeoecological data, we analyzed a comprehensive data set of 61 available genetic sequences retrieved from woolly rhinoceros fossils sampled across time and space. The data comprised mitochondrial DNA (mtDNA) control region sequences, a non-coding area with a high substitution rate that is ideal for inferring phylogeographic patterns. The data were analyzed to (i) investigate the distribution of genetic diversity across time and space, which has not previously been done; and (ii) associate patterns of mtDNA diversity and differentiation with isotopic variation.

2. Material and methods

2.1. Radiocarbon and stable isotope data

We present 192 new δ^{13}C and δ^{15}N measurements from woolly rhinoceros bone and tooth specimens (Supplementary Table 1), determined by isotope ratio mass spectrometry (CF-IRMS). These measurements were generated during ^{14}C radiocarbon dating of fossils for two previous studies (Lorenzen et al., 2011; Stuart and Lister, 2012). These two studies only reported ^{14}C ages, and not the corresponding δ^{13}C and δ^{15}N measurements. For the present study, we accessed and compiled the latter data. Although the woolly rhinoceros fossil records presented in (Lorenzen et al., 2011; Stuart and Lister, 2012) are not temporally or spatially exhaustive, and some geographic regions are underrepresented, they include a large number of specimens collected across time and space (Fig. 1).

We calibrated the ^{14}C dates retrieved from the previous publications using CALIB 8.2 (Stuiver et al., 2021) and the IntCal20 (Reimer et al., 2020) calibration curve. Unless otherwise stated, dates are reported as calibrated years before present (cal yr BP). Dates reported as infinite correspond to samples where the ^{14}C content was too small to produce a finite radiocarbon age. The samples ranged in age from infinite to 14,040 cal yr BP. The spatial distribution of the material spans northern Eurasia, with records from Spain to NE Siberia (Fig. 1).

Radiocarbon dating and isotopic measurements of samples were conducted at Oxford Radiocarbon Accelerator Unit (University of Oxford; OxA codes) and Aarhus AMS Center (University of Aarhus; AAR codes). At Oxford Radiocarbon Accelerator Unit, δ^{13}C and δ^{15}N were determined following the combustion/recycling protocol described in Brock et al., (2010). At Aarhus AMS Center, δ^{13}C and δ^{15}N were determined following the protocols described in Olsen et al. (2010)). Reliability of the stable isotopic values was established by measuring the atomic C:N ratio. All our samples fell within the accepted range of 2.9–3.6 (DeNiro, 1985; Ambrose, 1990).

To increase the number and range of δ^{13}C and δ^{15}N records in our analysis, we compiled a range-wide database of available δ^{13}C and δ^{15}N stable isotope records for woolly rhinoceros (Supplementary Table 1). We used Google Scholar to perform a

literature search with the terms "woolly rhinoceros" and "stable isotopes", and "*Coelodonta antiquitatis*" and "stable isotopes". We recovered data for 94 specimens, derived from ten published studies and spanning the species' range (Bocherens et al. 1995, 1996, 1997, 2005, 2011, 1996, 2005; Higham et al., 2006; Jacobi et al. 2006, 2007, 2009, 2007; Kirillova et al., 2015b; Kuc et al., 2012; Yates et al., 2017). All previously published data represented samples dated >28,660 cal yr BP. Our final dataset represented 286 samples (Fig. 1).

To contextualize the woolly rhinoceros isotopic data with other contemporary large herbivores, we performed a literature search and compiled $\delta^{13}C$ and $\delta^{15}N$ data for five other mammoth steppe species from Eurasia: horse, musk ox, reindeer, saiga, and woolly mammoth (Supplementary Table 2). Paleoecological inference based on $\delta^{13}C$ and $\delta^{15}N$ data is highly influenced by regional environmental characteristics, and large isotopic differences have been observed for $\delta^{13}C$ and $\delta^{15}N$ between the North American and Eurasian regions of the mammoth steppe (Szpak et al., 2010). As woolly rhinoceroses were only present in Eurasia, we omitted North American records for the other species.

2.2. Stable isotope analysis

To investigate temporal variation in the isotopic signature of woolly rhinoceroses and other megaherbivores, we divided the isotopic records into three time bins (Fig. 1), following Kuitems et al., (2019): pre-LGM (>24,600 ^{14}C yr BP/> 28,660 cal yr BP), LGM (24,600–17,000 ^{14}C yr BP/28,660–20,520 cal yr BP), and post-LGM (<17,000 ^{14}C yr BP/< 20,520 cal yr BP). The post-LGM cut-off date corresponds to 12,135 ^{14}C yr BP or 14,040 cal yr BP, the age of the youngest woolly rhinoceros specimen in our dataset. The sample size of each time bin was: pre-LGM n = 215, LGM n = 32, post-LGM n = 39 (Table 1).

To accommodate for differences in fossil chronology across Eurasia (such as the later survival of woolly rhinoceros in NE Siberia), and the environmental heterogeneity of Eurasia during the Late Pleistocene, we divided the data into four geographic regions: (i) western and central Europe (n = 97); (ii) European Russia, Urals and Kazakhstan (n = 57); (iii) southern and central Siberia and China (n = 46); and (iv) north-east Siberia (n = 86, Table 1). To simplify, we refer to these regions as W/C Europe, E Europe/Urals (as we only have one sample from Kazakhstan), S/C Siberia, and NE Siberia, respectively.

Stable isotopes were retrieved from both bone and tooth. The isotopic signature in bone material provides information on the average diet of an individual in the years preceding death (Hedges et al., 2007; Hobson and Clark, 1992). In contrast, data from mammalian tooth collagen corresponds to the early years of an individual's life, depending on the chronology of tooth development for the species in question (DeNiro, 1985; Bocherens, 2015). Furthermore, their $\delta^{15}N$ signature may reflect the suckling ^{15}N-enriched composition (DeNiro, 1985; Fizet et al., 1995; Bocherens and Drucker, 2013). We have no direct information on the weaning age of woolly rhinoceros, but infer a weaning age of 18 months based on the average age of weaning of a number of extant rhinoceros species (e.g. Owen-Smith, 1974; Osthoff et al., 2008; Gimmel et al., 2018). We do not have information on the age of the individuals used in this study, and assume all samples analyzed belonged to adult individuals.

For the purposes of our analysis, we assumed that the stable isotope composition of bone and tooth collagen are comparable, albeit systematic differences in $\delta^{13}C$ and $\delta^{15}N$ isotopic abundances between bone and dentine have been recognized in some mammals. For instance, lower $\delta^{15}N$ values in bone compared to dentine have been measured in carnivores such as bears and hyenas (Bocherens et al., 1997; Bocherens, 2015), or in herbivores such as reindeer (Fizet et al., 1995). For the species where the isotopic differences between bone and tooth have been directly identified and quantified, $\delta^{13}C$ and $\delta^{15}N$ data are adjusted before comparing bone and tooth isotopic values. However, there has been no systematic study characterising possible $\delta^{13}C$ and $\delta^{15}N$ isotopic differences between bone and tooth in woolly rhinoceros, and our data have thus not been corrected. We are aware of the bias that this might introduce to our data. However, assuming the correction factor for woolly rhinoceros is similar to estimates from other herbivore species, such as reindeer ($\delta^{13}C$ = 0.2‰–0.5‰ and $\delta^{15}N$ = 0.7‰–2‰, lower in bone than in dentine, Fizet et al., 1995), the skeletal element variation in our data set is less than the variation we detect among individuals across time bins and geographic regions.

Groups (representing time or space) with low sample size (n < 30) were tested for normality using the Shapiro-Wilkinson test. As the data distribution for some of these groups was not normal, we chose to use non-parametric testing for all analyses comparing isotopic signatures for different time bins and geographic regions. The Kruskal-Wallis test was used to determine statistical differences for each time bin among geographic regions.

To further detect differences between pairs of time bins and/or geographic regions, we used the post-hoc Kruskal Conover test applying the Bonferroni correction to control for Type I errors. Statistical data analysis was conducted in RStudio (Team RStudio, 2018) using the packages nortest (Gross and Ligges, 2015) and

Table 1
Summary of $\delta^{13}C$ and $\delta^{15}N$ values of the 286 woolly rhinoceros specimens analyzed in this study. The time bins were defined as: pre-LGM (>24,600^{14}C yr BP/> 28,660 cal yr BP), LGM (24,600–17,000^{14}C yr BP/28,660–20,520 cal yr BP), and post-LGM (<17,000^{14}C yr BP/< 20,520 cal yr BP). Number of specimens in each temporal/spatial bin is indicated in parenthesis.

Time bin (n)	Region (n)	$\delta^{13}C$ (‰)					$\delta^{15}N$ (‰)				
		Min	Max	Median	Mean	sd	Min	Max	Median	Mean	sd
pre-LGM (215)	W/C Europe (90)	−22.5	−18.1	−20	−20	0.7	0.7	11.5	5.3	5.3	1.8
	E Europe/Urals (34)	−20.8	−18.6	−19.5	−19.5	0.5	2.6	9.8	5.1	5.4	1.8
	S/C Siberia (26)	−20.5	−18.5	−19.6	−19.6	0.6	3	9.1	6.6	6.1	1.5
	NE Siberia (65)	−22.7	−19.5	−20.6	−20.6	0.6	2.6	10.8	6.6	6.7	1.9
LGM (32)	W/C Europe (3)	−19.8	−19.4	−19.6	−19.6	0.2	2.8	4.6	4.1	3.8	0.9
	E Europe/Urals (6)	−19.6	−19	−19	−19.1	0.2	4.4	8.8	5	5.5	1.7
	S/C Siberia (16)	−20.1	−18.4	−19.1	−19.1	0.5	3.1	10.3	4.9	5.2	1.8
	NE Siberia (7)	−20.7	−19.3	−20.1	−20	0.6	2.8	10.6	6.8	6.2	2.6
post-LGM (39)	W/C Europe (4)	−20.1	−19.8	−20	−20	0.1	2.6	4	3	3.1	0.6
	E Europe/Urals (17)	−20.6	−19	−19.8	−19.7	0.5	1.9	11.4	3.2	3.9	2.4
	S/C Siberia (4)	−20.4	−18.6	−19.8	−19.7	0.9	4.2	8.2	4.8	5.5	1.9
	NE Siberia (14)	−22.4	−19.7	−20.2	−20.3	0.7	2.3	9.5	6.7	6.3	2.7

PMCMR (Pohlert and Pohlert, 2018). Significant differences were reported at the 95% confidence level or p-value of 0.05.

Bivariate plots and boxplots were performed in RStudio (Team RStudio, 2018) using the package ggplot2 (Wickham, 2011). Summary statistics were obtained in RStudio. Multispecies comparisons were also performed using SIBER (Jackson et al., 2011), this R package was used to estimate and compare the Standard Ellipse Area (SEA) as a proxy for isotopic niche range.

2.3. DNA data compilation and analysis

To contextualize the stable isotope data and evaluate genetic changes across time and space, we compiled all available mtDNA control region sequences of woolly rhinoceros published to date (Lorenzen et al., 2011; Lord et al., 2020). Due to a large amount of missing data for the control region locus, eight of the 14 sequences from Lord et al., (2020) were not included in our analysis (Supplementary Table 3). We did not include the mtDNA sequence published in Willerslev et al. (2009), as the sample was not dated.

The final dataset comprised 61 mtDNA control region sequences; 35 of these samples were also represented in the stable isotope analysis (Supplementary Table 3). Sequences were aligned in Geneious (Kearse et al., 2012), and the length of the final alignment used in our analysis was 541 base-pairs (bp). We generated a haplotype network using the median-joining (Bandelt et al., 1999) algorithm implemented in the program PopART v1.7 (Leigh and Bryant, 2015).

To estimate a phylogeny, we used BEAST v.1.10.4 (Drummond et al., 2012) using the radiocarbon dates of the sequences to estimate a mutation rate and divergence times. This analysis was performed using the same dataset as for the haplotype network. We used a coalescent constant size model, as data were from a single species, and applied a strict clock. The clock rate was set to a normal distribution with an initial value of 6.1×10^{-9} substitutions/site/year, a mean value of 6.1×10^{-9}, and a standard deviation of 0.01 as in Lord et al., (2020). As estimated in PartitionFinder (Lanfear et al., 2012), we used the model HKY + I + G for all the codons of the control region.

All BEAST analyses were run in two independent MCMC chains of 1×10^{7}generations each, sampling trees and model parameters every 1×10^{3} generations. Tracer v1.6 (Rambaut et al., 2018) was used to combine and inspect the results of each run and to determine the convergence of each parameter, all of which had ESS values > 200. We identified the Maximum Clade Credibility (MCC) tree in TreeAnnotator v1.8.0, and visualized and graphically edited the MCC tree using Figtree.

The covariation of stable isotopes and haplogroups was also explored. A bivariate plot was performed in RStudio (Team RStudio, 2018) using the package ggplot2 (Wickham, 2011). A cluster dendrogram was generated using the R package cluster (Maechler, 2019). For this, we applied the Euclidean distance method algorithm with Ward's minimum variance criterion to minimize the total within-cluster variance. We set the number of clusters to three, equivalent to the number of haplogroups recovered in the phylogenetic analysis.

3. Results

3.1. Stable isotope analysis: woolly rhinoceros

Summary statistics of woolly rhinoceros stable isotope measurements were compiled in Table 1 and visually explored in Figs. 2–4 δ^{13}C values ranged from −22.7‰ to −18.1‰, with an average value of −19.9 ± 0.71‰. δ^{15}N values ranged from +0.7‰ to +11.5‰, with an average value of +5.7 ± 2.04‰. Summary statistics indicated a smaller range of variation for δ^{13}C than δ^{15}N.

Fig. 2A shows variation in δ^{13}C through time. We detected an increase in δ^{13}C starting ~34 cal kyr BP, which peaked at the onset of the LGM ~27 cal kyr BP, with a subsequent decline. We further explored differences in δ^{13}C within the three time bins using bivariate plots, and found higher average δ^{13}C during the LGM than for the other two time bins (Fig. 3). Statistical testing showed significant differences in average δ^{13}C between pre-LGM and LGM ($p < 0.001$), and between LGM and post-LGM ($p = 0.003$).

We investigated the influence of time on δ^{13}C within each of the four geographic regions (Fig. 4A). For three regions (excluding W/C Europe), we detected significant changes in average δ^{13}C over time (p-values: E Europe/Urals: $p = 0.02$; S/C Siberia: $p = 0.03$; NE Siberia: $p = 0.008$), with higher values during the LGM. Within each time bin, we identified differences in isotopic values across regions (Fig. 4A, Supplementary Table 4).

For δ^{15}N, we observed a gradual decline starting at the onset of the LGM ~27 cal kyr BP (Fig. 2B). When we split the range-wide dataset into three time bins, statistical testing showed significant differences in δ^{15}N between pre-LGM and post-LGM ($p = 0.002$) (Fig. 3). When the data were further investigated across time for each geographic region, we detected significant continuous declines in average δ^{15}N over time for two regions (p-values: W/C Europe: $p = 0.010$, E Europe/Urals: $p = 0.004$), but not for S/C and NE Siberia (Fig. 4B).

For pre-LGM, pairwise comparisons between regions showed significant differences between NE Siberia and both W/C Europe and E Europe/Urals (Fig. 4B, Supplementary Table 4). For LGM, we did not identify any differences in δ^{15}N between regions. For post-LGM, NE Siberia δ^{15}N differed significantly from E Europe/Urals.

3.2. Stable isotope analysis: other herbivores

To contextualize woolly rhinoceros isotopic variation, we compared the data with stable isotope records from five co-distributed herbivore species. To make the data directly comparable across time and space, we restricted the geographic distribution of the data to Eurasia (Supplementary Table 2). Bivariate and boxplots of the data divided by species and by time bin correspond to Figs. 5 and 6. Graphical exploration and statistical testing indicated that pre-LGM δ^{13}C and δ^{15}N of rhinoceros differed from all the other species surveyed (Figs. 5 and 6, Supplementary Table 5). Rhinoceros LGM δ^{13}C and δ^{15}N were similar to saiga. Post-LGM rhinoceros δ^{13}C and δ^{15}N values were similar to musk ox.

To estimate species isotopic ranges, we used the Standard Ellipse Area (SEA) function implemented in SIBER (Supplementary Table 6). For pre-LGM, saiga had the largest isotopic range (SEA = 5.16), followed by rhinoceros (SEA = 4.25). For LGM, we observed a decline in isotopic range for four species, except mammoth (SEA = 2.91) and saiga (SEA = 5.30). For rhinoceros, SEA was reduced to 3.65, still remaining second largest after saiga. For post-LGM, rhinoceros had the largest SEA (SEA = 4.98), with an increase in ellipse area from the LGM (LGM SEA = 3.65). For rhinoceros, post-LGM isotopic range returned to pre-LGM values, albeit with overall lower δ^{15}N values.

3.3. DNA analysis

We identified three haplogroups (A-C) in the mtDNA control region data (Fig. 7, Supplementary Figure 1, and Supplementary Table 3). The alignment contained 66 segregating sites; haplogroups A and B differed from each other at two nucleotide positions, and haplogroups B to C at six nucleotide positions.

Haplogroup A was only found in S/C and NE Siberia; it was present in NE Siberia pre-LGM, in S/C Siberia during LGM, and in

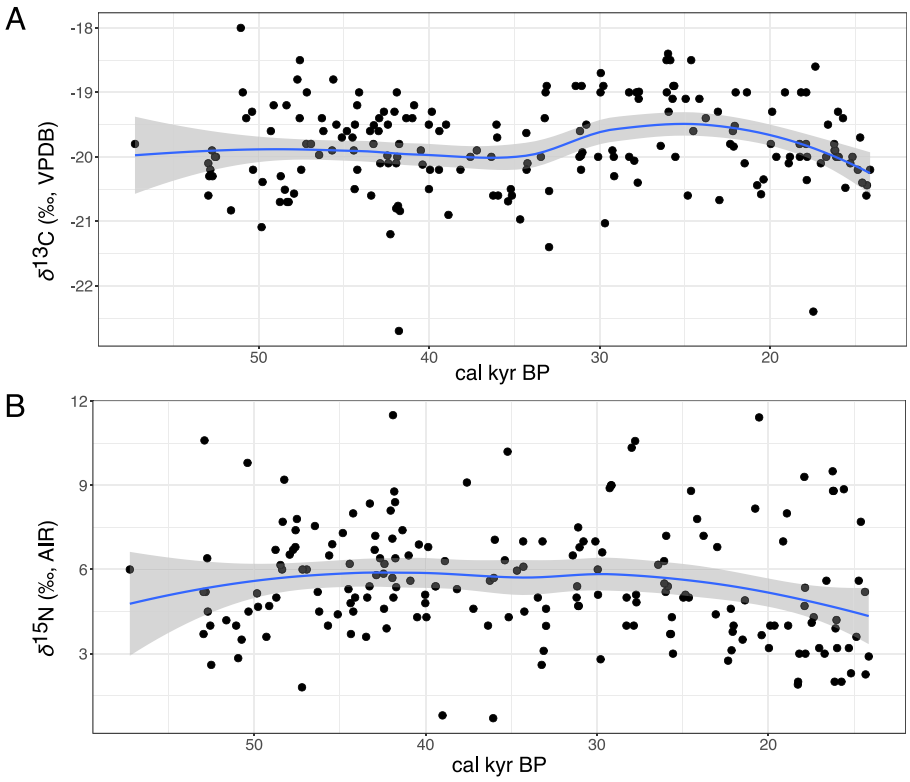

Fig. 2. Temporal variation in (A) $\delta^{13}C$ and (B) $\delta^{15}N$ isotopic values across the 286 woolly rhinoceros specimens analyzed in this study. Local regression curves were estimated using the LOESS (locally estimated scatterplot smoothing) method as implemented in ggplot2 (Wickham, 2011).

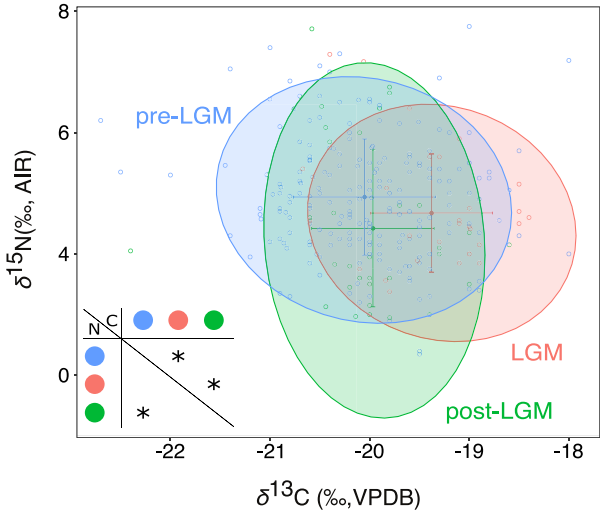

Fig. 3. Bivariate plot of $\delta^{13}C$ and $\delta^{15}N$ isotopic values across the 286 woolly rhinoceros specimens analyzed in this study. Data were divided into three time bins: pre-LGM (n = 215), LGM (n = 32), and post-LGM (n = 39). Ellipses represent 0.95 confidence levels. Crosses represent mean value±s.d. for each time bin. Matrix represents pairwise comparison of differences in $\delta^{13}C$ (above diagonal) and $\delta^{15}N$ (below diagonal); significant differences between time bins are indicated with an asterisk. (For interpretation of the references to colour in this figure legend, the reader is referred to the Web version of this article.)

both regions post-LGM.

Haplogroup B extended from southern Russia to NE Siberia: pre-LGM, haplogroup B was present in S/C and NE Siberia; during the LGM, we identified haplogroup B in samples from southern Russia, S/C Siberia, and NE Siberia; post-LGM, the haplogroup was present in E Europe/Urals and NE Siberia.

Haplogroup C was present across the species range in pre-LGM, extending from central Europe to NE Siberia. During LGM, haplogroup C remained in S/C and NE Siberia. Post-LGM, only woolly rhinoceroses from E Europe/Urals carried this haplogroup.

We also explored the covariation of stable isotopes and haplogroups. We could not identify any relationship between them (Supplementary Figure 2).

4. Discussion

We analyzed $\delta^{13}C$ and $\delta^{15}N$ stable isotope data from 286 woolly rhinoceros specimens sampled across Eurasia, spanning over 45 kyr of evolutionary history. Our analyses revealed variation across geographic regions; S/C and NE Siberia showed stability in isotopic composition across time, in contrast with other regions, which experienced variation in $\delta^{15}N$. We found no geographic structuring among the 61 mtDNA sequences analyzed, but did recover three well-differentiated haplogroups with overlapping distributions, all of which showed a signal of expansion during the LGM.

4.1. Temporal variation in $\delta^{13}C$ within and among regions

Across samples, we found an average $\delta^{13}C$ value of −19.9‰, indicating woolly rhinoceroses had a diet dominated by C_3 plants (Bocherens, 2003); this is expected in herbivores from cold and temperate climates. We detected significant changes in average $\delta^{13}C$ across time bins; between pre-LGM and LGM, and between LGM and post-LGM (Fig. 3).

Although values remained within the C_3 diet range, we found higher $\delta^{13}C$ during the LGM. An increase in plant $\delta^{13}C$ has been associated with water stress (Farquhar et al., 1982; Stewart et al.,

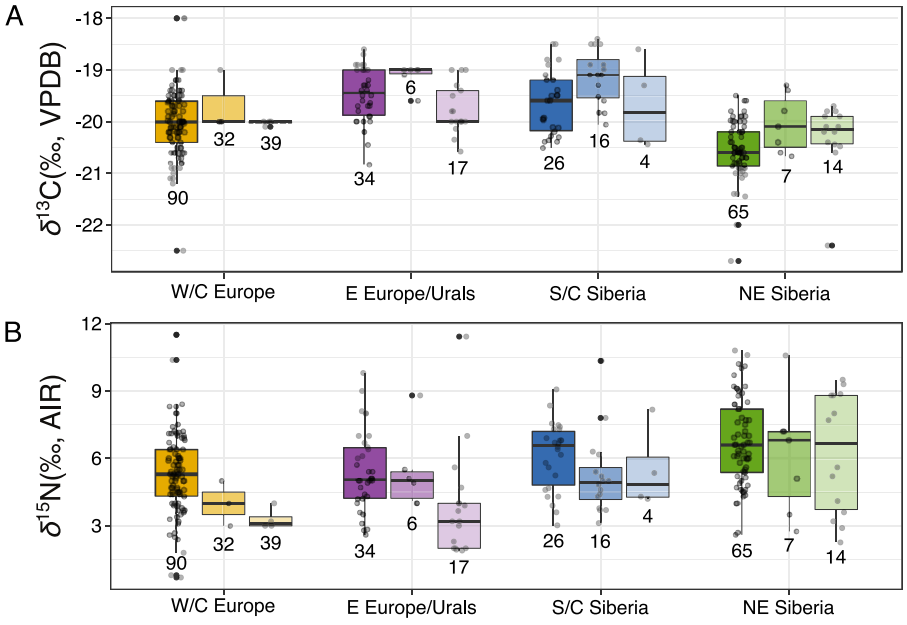

Fig. 4. Boxplots showing spatial and temporal variation in (A) $\delta^{13}C$ and (B) $\delta^{15}N$ in woolly rhinoceroses. For each region, boxplots are organized in time bins from left to right: pre-LGM, LGM, and post-LGM. Sample sizes are indicated below each box plot. Box plots represent median, upper, and lower quartile, and whiskers represent highest and lowest value.

1995). Drier environmental conditions during the LGM have been inferred across Eurasia based on paleoenvironmental proxies (Hubberten et al., 2004), and are further supported by bioclimatic models, which show the expansion of tundra and simultaneous reduction of boreal and temperate forests 21 ka BP (Hoogakker et al., 2016).

Post-LGM, average $\delta^{13}C$ declined, reaching values similar to pre-LGM (Fig. 3). Plants from wet environments display lower $\delta^{13}C$ than those from dry environments (Wooller et al., 2007), and our findings of an overall decline in $\delta^{13}C$ after the LGM may reflect an increase in moisture due to precipitation and degrading permafrost during the Late Glacial (Rabanus-Wallace et al., 2017).

We identified significant changes in $\delta^{13}C$ over time for three of the four geographic regions (excluding W/C Europe, Fig. 4A). In the E Europe/Urals and S/C Siberia, we observed a decrease in $\delta^{13}C$ between LGM and post-LGM. In NE Siberia, we detected an increase in $\delta^{13}C$ from pre-LGM to LGM, which remained stable during the post-LGM.

Woolly rhinoceroses ranged across the Eurasian mammoth steppe, a heterogeneous environment encompassing a mosaic of varied local environments (Szpak et al., 2010). This was reflected in our pairwise comparisons between regions, which indicated spatial differences in $\delta^{13}C$ (Supplementary Table 4); for instance, we observed lower average $\delta^{13}C$ in woolly rhinoceroses from NE Siberia compared with the three other regions, in particular compared to E Europe/Urals and S/C Siberia during pre-LGM and LGM (Fig. 4A, Table 1). Lower $\delta^{13}C$ has previously been associated with lower annual temperatures (Szpak et al., 2010), and this may also be the case for NE Siberia. However, this finding is unexpected, as NE Siberia was characterized by consistently arid conditions throughout the Late Pleistocene (Sher et al., 2005), and plants from dry environments have higher $\delta^{13}C$ (Wooller et al., 2007), which should be reflected in the $\delta^{13}C$ composition of herbivores. Furthermore, the observed regional differences could be driving some of the overall patterns detected in our dataset; for example, the overall higher $\delta^{13}C$ values during the LGM could be caused by the higher $\delta^{13}C$ from E Europe/Urals and S/C Siberia during that period.

4.2. Temporal variation in $\delta^{15}N$ within and among regions

Our range-wide dataset showed significant changes in $\delta^{15}N$ over time. A significant, gradual decline in $\delta^{15}N$ was observed across the three time bins in two of the geographic regions (W/C Europe and E Europe/Urals, Fig. 4B). The decline observed from pre-LGM to LGM in S/C Siberia was not significant. A similar pattern of continuous decline in $\delta^{15}N$ from the Late Pleistocene until after the LGM has been observed in European reindeer, attributed to the climatic cooling that culminated during the LGM (Stevens et al., 2008). The post-LGM decline in $\delta^{15}N$, which is also reported in reindeer, has been linked to an increase in moisture due to precipitation and degrading permafrost (Drucker et al. 2003, 2011, 2011; Stevens et al., 2008). These more recent environmental changes have been attributed a major role in the Late Pleistocene and Holocene megafauna extinctions (Rabanus-Wallace et al., 2017; Drucker et al., 2018).

Between regions, we observed some temporal differences in $\delta^{15}N$ (Fig. 4B): pre-LGM, average $\delta^{15}N$ in NE Siberia was significantly higher than in W/C Europe and E Europe/Urals; LGM and post-LGM, the decline in average $\delta^{15}N$ observed in other regions was not observed in NE Siberia, which continued to have high average $\delta^{15}N$.

Regional differences in $\delta^{15}N$ may be driven by environmental and vegetational factors. For example, water stress and moisture influence nitrogen isotopic composition, increasing and lowering $\delta^{15}N$, respectively. Differences in $\delta^{15}N$ composition have also been identified based on the ecosystem where plants grow; for instance, grasses from heath, fellfield, and boreal forest have distinct $\delta^{15}N$ signatures (Bocherens, 2003). Thus, it is not unexpected that we find differences in woolly rhinoceroses $\delta^{15}N$ among regions, which were heterogeneous (Szpak et al., 2010). Moreover, the forms and concentrations of nitrogen that are present in the soil (i.e., mineralized or organic N) will influence the mechanisms by which plants obtain nitrogen for growth. Specifically, the interactions that plants form with symbiotic fungi (mycorrhizae) are significant, as

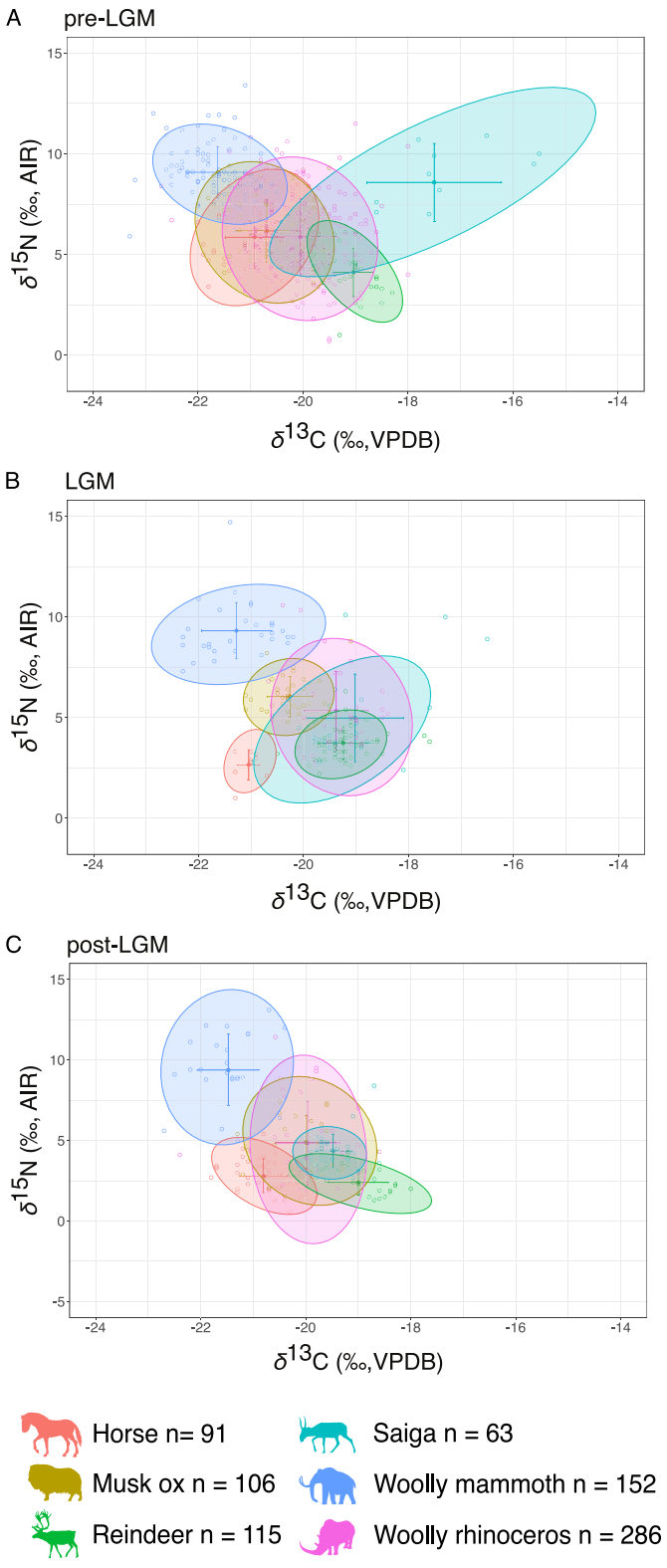

Fig. 5. Bivariate plot of $\delta^{13}C$ and $\delta^{15}N$ isotopic composition of woolly rhinoceroses and other contemporary megaherbivores from Eurasia. Ellipses represent 0.95 confidence levels. Crosses represent mean value±s.d. for each species. Panels represent three time bins: (A) pre-LGM, (B) LGM, and (C) post-LGM. Sample sizes for each species are indicated. Horse, musk ox, reindeer, and woolly rhinoceros silhouettes: license Public Domain Dedication 1.0; saiga silhouette: Andrey Giljov, license CC-BY-SA-4.0 (https://creativecommons.org/licenses/by-sa/4.0/deed.en); woolly mammoth silhouette: Zimices, license CC BY-NC-3.0 (https://creativecommons.org/licenses/by-nc/3.0/). (For interpretation of the references to colour in this figure legend, the reader is referred to the Web version of this article.)

different mycorrhizal types have varying capacities to convert organic N into mineralized N, and these capacities are strongly correlated with $\delta^{15}N$ values in both fungi and their plant partners (Hobbie and Högberg, 2012).

The continuous decline in average $\delta^{15}N$ observed in W/C Europe and E Europe/Urals may reflect changes in the nutrient status of the soil, such as increasing levels of recalcitrant organic nitrogen and decreasing levels of mineralized nitrogen (e.g., NH_4+ and NO_3-) that are readily available for plants. If the entire system becomes more dependent on fungi to process organic N and deliver it to plants, the proteolytic capabilities of those fungi impart very low $\delta^{15}N$ values on the plants that receive the mineralized nitrogen (Hobbie and Högberg, 2012).

The reduction in the number of herbivores in the landscape, which has been described in previous studies (e.g. Lorenzen et al., 2011; Lister & Stuart, 2019), may also have played a role in the decline in $\delta^{15}N$ values. Herbivores are effective recyclers of nitrogen, by depositing it back into the soil as urine and feces. An increase in the abundance of herbivores would lead to more rapid nitrogen cycling, providing more mineralized nitrogen available for plants (McNaughton, 1979). Thus, there could have been an important feedback loop that was being altered in areas where megafauna was declining.

4.3. Temporal stability in $\delta^{15}N$ in NE Siberia

The fossil record, based on published radiocarbon dates, shows the continuous presence of woolly rhinoceroses in NE Siberia from >50 cal kyr BP until their extinction ~14 cal kyr BP (Stuart and Lister, 2012). The region was home to the last surviving population of woolly rhinoceros, which survived there ~1000 years later than elsewhere.

Later persistence of open vegetation, which may have presented more suitable habitat and food resources, has been suggested to have played a role in the later survival of woolly rhinoceroses in NE Siberia (Stuart and Lister, 2012). This is supported by palaeoecological proxies, which show environmental stability in NE Siberia throughout the Late Pleistocene (Clark et al., 2012; Jørgensen et al., 2012; Willerslev et al., 2014), and is further supported by our findings.

We found no significant changes in $\delta^{15}N$ over time in NE Siberia (Fig. 4B). This pattern indicates dietary stability, suggesting woolly rhinoceroses fed on resources with similar isotopic compositions through time. Such a scenario would require a stable environment. Temporal stability in $\delta^{15}N$ in NE Siberia has also been observed in musk ox from Taimyr and in woolly mammoth from NE Siberia (Raghavan et al., 2014; Kuitems et al., 2019), suggesting broad-scale environmental stability, rather than a species-specific pattern.

Environmental stability may have been key to the late survival of woolly rhinoceroses (and other species) in the region. In woolly mammoths, isotopic stability has been reported in both mainland NE Siberia and on Wrangel Island. Both areas were continuously inhabited by the species until their mainland and island extinctions, respectively (Arppe et al., 2019; Kuitems et al., 2019). The survival of mammoths on Wrangel Island well into the Holocene is attributed to dietary stability, and to surviving populations feeding on resources with similar isotopic composition as the Late Pleistocene mammoth population in NE Siberia (Arppe et al., 2019; Kuitems et al., 2019). We suggest a similar scenario in woolly rhinoceroses, where the NE Siberian population retained a stable diet throughout the Late Pleistocene, until its extinction.

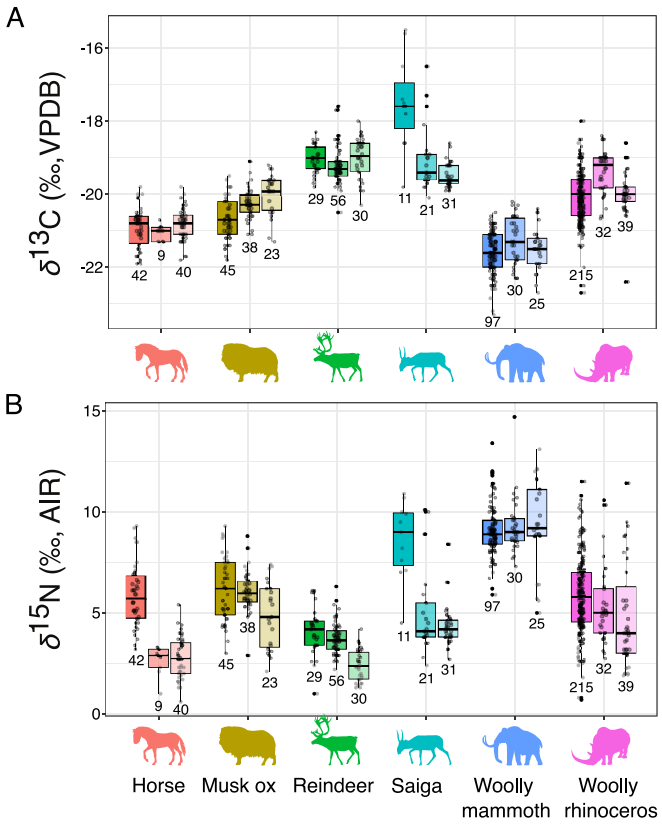

Fig. 6. Boxplots representing isotopic variation over time for (A) $\delta^{13}C$ and (B) $\delta^{15}N$ in six Late Pleistocene megaherbivores. For each species, boxplots are organized from left to right: pre-LGM, LGM, and post-LGM. Sample sizes are indicated below each box plot. Box plots represent median, upper, and lower quartile, and whiskers represent highest and lowest value. Horse, musk ox, reindeer, and woolly rhinoceros silhouettes: license Public Domain Dedication 1.0; saiga silhouette: Andrey Giljov, license CC-BY-SA-4.0 (https://creativecommons.org/licenses/by-sa/4.0/deed.en); woolly mammoth silhouette: Zimices, license CC BY-NC-3.0 (https://creativecommons.org/licenses/by-nc/3.0/).

4.4. Isotopic niche partitioning among herbivores

In contemporaneous herbivores, interspecific differences in isotopic composition have been associated with species-specific digestion processes, dietary specialization, and niche partitioning (Drucker et al., 2003; Bocherens et al., 2015). The woolly rhinoceros is considered a grazer, primarily feeding on grass and grass-like plants (Boeskorov et al., 2011; Rivals and Lister, 2016; Stefaniak et al., 2020). Morphological and genetic stomach content analysis furthermore indicates the presence of herbaceous plants (sagebrushes and forbs) (Boeskorov et al., 2011; Willerslev et al., 2014).

Despite being seen as a specialized grazer, woolly rhinoceroses exhibited variable isotopic values that overlap with other large herbivores through time and space (Figs. 5 and 6). This suggests a higher ecological flexibility than expected, and is supported by other studies on woolly rhinoceros diet (Kosintsev et al., 2019; Stefaniak et al., 2020). We found the isotopic composition of woolly rhinoceros overlapped with musk ox and saiga, albeit during different time bins. Woolly rhinoceros pre-LGM average $\delta^{13}C$ and $\delta^{15}N$ differ from the other analyzed herbivores, with intermediate average $\delta^{13}C$ values. During the LGM, woolly rhinoceros average $\delta^{13}C$ and $\delta^{15}N$ were similar to saiga, and post-LGM values were similar to musk ox; all three species are grazers. Saigas feed predominantly on grasses and chenopods (Hopkins et al., 2013). Musk ox are classified as grazers based on the anatomy of their digestive system (Knott et al., 2004), and they feed primarily on grasses, sedges, and willows (Raghavan et al., 2014). The isotopic affinity of woolly rhinoceroses to these two species was not constant across time bins. Standard Ellipse Analysis shows that patterns of variation in isotopic range across time bins is species-specific (Fig. 5). Thus, it is expected that isotopic niches changed across time periods, reflecting species-specific responses to environmental change.

Overall, our results showed that woolly rhinoceros $\delta^{13}C$ values are higher than horse and woolly mammoth, the two other monogastric hindgut fermenters included in our analysis, and we suggest this may reflect ecological niche partitioning or even dietary competition between woolly rhinoceros and woolly mammoth (Figs. 5 and 6). Such dietary competition, and at times

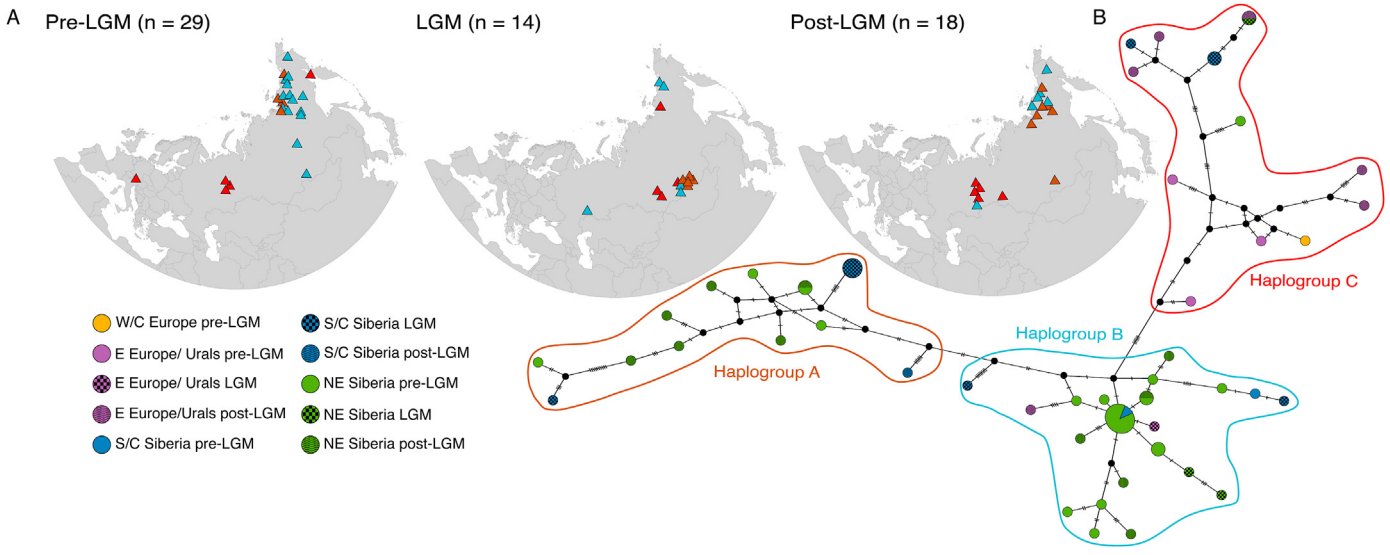

Fig. 7. Mitochondrial haplotype network of 61 published control region sequences. (A) Geographic distribution of haplotypes across three time bins: pre-LGM, LGM, and post-LGM. Colours correspond to haplogroups, shown as polygons in panel B; haplogroup A = brown, haplogroup B = blue, and haplogroup C = red. (B) Haplotype network. Circles correspond to haplotypes, colours correspond to geographic origin of samples, and pattern corresponds to time bin (see legend). Circle size indicates number of samples per haplotype. (For interpretation of the references to colour in this figure legend, the reader is referred to the Web version of this article.)

ecological exclusion, has been demonstrated in ecological studies of Asiatic elephants and Indian rhinoceroses (Pradhan et al., 2008), and of African elephants and black rhinoceroses (Landman et al., 2013).

4.5. mtDNA shows absence of phylogeographic structuring and LGM lineage expansion

Previous studies have used mtDNA to address the phylogenetic placement of woolly rhinoceros relative to other rhino species (Orlando et al., 2003; Willerslev et al., 2009), to explore the mitogenomics of NE Siberian woolly rhinoceroses (Lord et al., 2020), and to elucidate the demographic history of the species (Lorenzen et al., 2011; Lord et al., 2020). However, a comprehensive phylogeographic study across time and space has so far been lacking. To investigate spatial and temporal patterns of genetic variation across Eurasia, we compiled and analyzed 61 radiocarbon dated DNA sequences from Late Pleistocene woolly rhinoceroses.

We identified three well-differentiated mtDNA haplogroups (A-C) (Fig. 7). Despite the haplotype network analysis separating haplogroups A and B by only two nucleotide differences, our BEAST analysis showed strong posterior support differentiating them (Supplementary Figure 1). Our analysis included six control region sequences from Lord et al. (2020), which in that study, based on entire mitochondrial genomes, were assigned to woolly rhinoceros mitogenome clade 1 ($n = 2$) and clade 2 ($n = 4$). Mitogenome clade 1 corresponded to our haplogroup B, and mitogenome clade 2 corresponded to our haplogroup A, further supporting our haplogroup division based on the shorter control region sequences.

The mtDNA control region haplogroups were not geographically structured in time and/or space, and extended from Central Europe to NE Siberia; the only mtDNA sequence included from W/C Europe grouped in haplogroup C (Fig. 7). During the pre-LGM, haplogroup A was present in NE Siberia only, with an LGM expansion into S/C Siberia; the first appearance of haplogroup A in S/C Siberia was dated to 25,870 cal yr BP. A similar pattern was observed in haplogroup B; pre-LGM it was limited to S/C and NE Siberia, and expanded into E Europe/Urals during the LGM. The expansion of haplogroups A and B into new regions occurred at a time where demographic analysis of subsets of the data indicates an increase in population size (Lorenzen et al., 2011; Lord et al., 2020).

The presence of spatially overlapping yet divergent haplogroups likely reflects the allopatric divergence of lineages, with subsequent population expansion leading to the distribution of woolly rhinoceros populations across northern Eurasia. Siberia harbored the highest levels of genetic diversity, and was the only area where all three haplogroups were found. However, DNA analysis of additional specimens from the western part of the species range are needed to confirm this pattern.

For other megaherbivore species, such as bison, high genetic diversity has also been identified in NE Siberia (Kirillova et al., 2015a; Massilani et al., 2016). Genetic data from wolves (*Canis lupus*) suggest Late Pleistocene populations likely originated and expanded from NE Siberia into Eurasia and North America (Loog et al., 2020). Climatic stability has been suggested as a possible explanation for this pattern of maintained genetic diversity in NE Siberia (Loog et al., 2020); a scenario supported by our study.

Demographic analysis of 55 of the 61 mtDNA sequences analyzed here showed changes in genetic connectivity through time, with increasing fragmentation prior to extinction leading to population isolation (Lorenzen et al., 2011). The phylogeographic pattern revealed in our analysis supports this hypothesis of a decline in connectivity over time; we observed some changes in the geographic distribution of haplogroups over time, although we did not detect a loss of mtDNA haplogroups from pre-LGM to post-LGM. Two of the youngest samples included in our study (dated to 14,390 and 15,340 cal yr BP) were from NE Siberia and represented haplogroups A and B, respectively (Fig. 7). The youngest haplogroup C sample was from E Europe/Urals and is dated to 16,390 cal yr BP.

Previous analysis of 14 mitochondrial genomes from NE Siberia also support lineage continuity from pre-LGM to post-LGM in this region (Lord et al., 2020). However, further data are needed to confirm this pattern, as inferences in (Lord et al., 2020) were based on a small number of individuals, with an overrepresentation of sequences from NE Siberia.

5. Implications for woolly rhinoceros extinction

We investigated a comprehensive $\delta^{13}C$ and $\delta^{15}N$ dataset of woolly rhinoceroses, and included the first 71 stable isotope records spanning the 15 kyr preceding species extinction. Our study underscores the applicability of combining range-wide stable isotope studies with ancient DNA analysis, to obtain a broader understanding of the evolutionary ecology of past populations. We uncovered ecological flexibility and geographic variation in woolly rhinoceros, and suggest spatial and temporal variation in isotopic composition was driven by environmental and vegetational factors. Our analysis showed Late Pleistocene stability in $\delta^{15}N$ in NE Siberia, which we suggest reflects long-term environmental stability that may have favoured the later survival of woolly rhinoceros in the region.

Our comparative analysis with contemporaneous herbivores suggested possible niche partitioning of woolly rhinoceroses. We detected temporal variation in the isotopic profile of woolly rhinoceroses compared with other herbivores, which further supports the ecological flexibility of the species.

Ancient DNA analyses showed a lack of geographic structure at the mitochondrial level, with divergent lineages overlapping in time and space, as has been shown with a more spatially and temporally limited dataset from NE Siberia (Lord et al., 2020). We did not detect lineage loss prior to species extinction.

Stable isotope analyses have been used to investigate causes of extinction in other herbivores. For woolly mammoths, isotopic evidence suggested either a population decline (due to human encroachment) allowing other species (horse) to occupy their niche (Drucker et al., 2015), or a niche change forced by climate-induced environmental change (Drucker et al., 2018). Our data did not support either of these scenarios in woolly rhinoceroses.

Radiocarbon chronologies and genetic data have correlated the extinction of woolly rhinoceroses with climatic and environmental factors (Lorenzen et al., 2011; Stuart and Lister, 2012; Lord et al., 2020). Demographic analysis based on genetic data has indicated an increase in population size ~30 cal kyr BP followed by demographic stability until ~18.5 cal kyr BP, where a decline in woolly rhinoceros population size started. Our results indicated that environmental stability enabled the late survival of woolly rhinoceroses in NE Siberia, and thus, environmental changes around the time of extinction may have had detrimental effects on the remaining populations. Pollen records for the region have documented a spread of shrub tundra communities and increased precipitation 13.5–12.7 cal kyr BP, compared to the open steppe-tundra community that was previously found in the region (until ~15 cal kyr BP) (Müller et al., 2009). We suggest the interplay between environmental instability and fragmentation/isolation of populations, as presented in Lorenzen et al. (2011), played a major role in the extinction of the woolly rhinoceroses.

Authors contributions

ARI: Data Curation, Formal analysis, Visualization, Writing - Original Draft. AML: Resources, Funding acquisition, Writing - Review & Editing. AJS: Resources, Funding acquisition. HB: Conceptualization, Formal analysis, Writing - Original Draft. PS: Writing - Original Draft, Conceptualization. EW: Resources, Funding acquisition, Writing - Review & Editing. EDL: Conceptualization, Funding acquisition, Writing - Original Draft.

Funding

The work was supported by Villum Fonden Young Investigator Programme, grant no. 13151 to EDL.

Declaration of competing interest

The authors declare that they have no known competing financial interests or personal relationships that could have appeared to influence the work reported in this paper.

Acknowledgements

We thank Edana Lord and Nic Dussex for granting pre-publication access to the mitochondrial genome sequences published in Lord et al., 2020), which were included in our analyses.

Appendix A. Supplementary data

Supplementary data to this article can be found online at https://doi.org/10.1016/j.quascirev.2021.106993.

References

Ambrose, S.H., 1990. Preparation and characterization of bone and tooth collagen for isotopic analysis. J. Archaeol. Sci. 17 (4), 431–451. https://doi.org/10.1016/0305-4403(90)90007-r.

Arppe, L., Karhu, J.A., Vartanyan, S., Drucker, D.G., Etu-Sihvola, H., Bocherens, H., 2019. Thriving or surviving? The isotopic record of the Wrangel Island woolly mammoth population. Quat. Sci. Rev. 222, 105884. https://doi.org/10.1016/j.quascirev.2019.105884.

Bandelt, H.J., Forster, P., Röhl, A., 1999. Median-joining networks for inferring intraspecific phylogenies. Mol. Biol. Evol. 16 (1), 37–48. https://doi.org/10.1093/oxfordjournals.molbev.a026036.

Bocherens, H., Fogel, M.L., Tuross, N., Zeder, M., 1995. Trophic structure and climatic information from isotopic signatures in Pleistocene cave fauna of southern England. J. Archaeol. Sci. 22 (2), 327–340. https://doi.org/10.1006/jasc.1995.0035.

Bocherens, H., Pacaud, G., Lazarev, P.A., Mariotti, A., 1996. Stable isotope abundances (^{13}C, ^{15}N) in collagen and soft tissues from Pleistocene mammals from Yakutia: implications for the palaeobiology of the Mammoth Steppe. Palaeogeogr. Palaeoclimatol. Palaeoecol. 126 (1–2), 31–44. https://doi.org/10.1016/s0031-0182(96)00068-5.

Bocherens, H., Billiou, D., Patou-Mathis, M., Bonjean, D., Otte, M., Mariotti, A., 1997. Paleobiological implications of the isotopic signatures (^{13}C, ^{15}N) of fossil mammal collagen in Scladina Cave (Sclayn, Belgium). Quat. Res. 48 (3), 370–380. https://doi.org/10.1006/qres.1997.1927.

Bocherens, H., 2003. Isotopic biogeochemistry and the palaeoecology of the mammoth steppe fauna. Deinsea 9 (1), 57–76.

Bocherens, H., Drucker, D.G., 2013. CARBONATE STABLE ISOTOPES. Terrestrial Teeth and Bones, 10.1016/b0-44-452747-8/00353-7.

Bocherens, H., Drucker, D.G., Billiou, D., Patou-Mathis, M., Vandermeersch, B., 2005. Isotopic evidence for diet and subsistence pattern of the Saint-Césaire I Neanderthal: review and use of a multi-source mixing model. J. Hum. Evol. 49 (1), 71–87. https://doi.org/10.1016/j.jhevol.2005.03.003.

Bocherens, H., Drucker, D.G., Bonjean, D., Bridault, A., Conard, N.J., Cupillard, et al., 2011. Isotopic evidence for dietary ecology of cave lion (*Panthera spelaea*) in North-Western Europe: prey choice, competition and implications for extinction. Quat. Int. 245 (2), 249–261. https://doi.org/10.1016/j.quaint.2011.02.023.

Bocherens, H., 2015. Isotopic tracking of large carnivore palaeoecology in the mammoth steppe. Quat. Sci. Rev. 117, 42–71. https://doi.org/10.1016/j.quascirev.2015.03.018.

Bocherens, H., Hofman-Kamińska, E., Drucker, D.G., Schmölcke, U., Kowalczyk, R., 2015. European bison as a refugee species? Evidence from isotopic data on Early Holocene bison and other large herbivores in northern Europe. PloS One 10 (2), e0115090. https://doi.org/10.1371/journal.pone.0115090.

Boeskorov, G.G., Lazarev, P.A., Sher, A.V., Davydov, S.P., Bakulina, N.T., Shchelchkova, et al., 2011. Woolly rhino discovery in the lower Kolyma River. Quat. Sci. Rev. 30 (17–18), 2262–2272. https://doi.org/10.1016/j.quascirev.2011.02.010.

Bonafini, M., Pellegrini, M., Ditchfield, P., Pollard, A.M., 2013. Investigation of the 'canopy effect' in the isotope ecology of temperate woodlands. J. Archaeol. Sci. 40 (11), 3926–3935. https://doi.org/10.1016/j.jas.2013.03.028.

Brock, F., Higham, T., Ditchfield, P., Ramsey, C.B., 2010. Current pretreatment methods for AMS radiocarbon dating at the Oxford radiocarbon accelerator unit (ORAU). Radiocarbon 52 (1), 103–112. https://doi.org/10.1017/s0033822200045069.

Clark, P.U., Shakun, J.D., Baker, P.A., Bartlein, P.J., Brewer, S., Brook, E., et al., 2012. Global climate evolution during the last deglaciation. Proc. Natl. Acad. Sci. Unit. States Am. 109 (19), E1134–E1142. https://doi.org/10.1073/pnas.1116619109.

Cooper, A., Turney, C., Hughen, K.A., Brook, B.W., McDonald, H.G., Bradshaw, C.J., 2015. Abrupt warming events drove Late Pleistocene Holarctic megafaunal turnover. Science 349 (6248), 602–606. https://doi.org/10.1126/science.aac4315.

DeNiro, M.J., 1985. Postmortem preservation and alteration of in vivo bone collagen isotope ratios in relation to palaeodietary reconstruction. Nature 317 (6040), 806–809. https://doi.org/10.1038/317806a0.

Drucker, D.G., Bocherens, H., Billiou, D., 2003. Evidence for shifting environmental conditions in Southwestern France from 33 000 to 15 000 years ago derived from carbon-13 and nitrogen-15 natural abundances in collagen of large herbivores. Earth Planet Sci. Lett. 216 (1–2), 163–173. https://doi.org/10.1016/s0012-821x(03)00514-4.

Drucker, D.G., Kind, C.J., Stephan, E., 2011. Chronological and ecological information on Late-glacial and early Holocene reindeer from northwest Europe using radiocarbon (^{14}C) and stable isotope (^{13}C, ^{15}N) analysis of bone collagen: case study in southwestern Germany. Quat. Int. 245 (2), 218–224. https://doi.org/10.1016/j.quaint.2011.05.007.

Drucker, D.G., Vercoutere, C., Chiotti, L., Nespoulet, R., Crépin, L., Conard, N.J., et al., 2015. Tracking possible decline of woolly mammoth during the Gravettian in Dordogne (France) and the Ach Valley (Germany) using multi-isotope tracking (^{13}C, ^{14}C, ^{15}N, ^{34}S, ^{18}O). Quat. Int. 359, 304–317. https://doi.org/10.1016/j.quaint.2014.11.028.

Drucker, D.G., Stevens, R.E., Germonpré, M., Sablin, M.V., Péan, S., Bocherens, H., 2018. Collagen stable isotopes provide insights into the end of the mammoth steppe in the central East European plains during the Epigravettian. Quat. Res. 90 (3), 457–469. https://doi.org/10.1017/qua.2018.40.

Drummond, A.J., Suchard, M.A., Xie, D., Rambaut, A., 2012. Bayesian phylogenetics with BEAUti and the BEAST 1.7. Mol. Biol. Evol. 29 (8), 1969–1973. https://doi.org/10.1093/molbev/mss075.

Farquhar, G.D., O'Leary, M.H., Berry, J.A., 1982. On the relationship between carbon isotope discrimination and the intercellular carbon dioxide concentration in leaves. Funct. Plant Biol. 9 (2), 121–137. https://doi.org/10.1071/PP9820121.

Fizet, M., Mariotti, A., Bocherens, H., Lange-Badré, B., Vandermeersch, B., Borel, J.P., Bellon, G., 1995. Effect of diet, physiology and climate on carbon and nitrogen stable isotopes of collagen in a Late Pleistocene anthropic palaeo ecosystem: Marillac, Charente, France. J. Archaeol. Sci. 22 (1), 67–79. https://doi.org/10.1016/s0305-4403(95)80163-4.

Gimmel, A., Hoby, S., Deillon, L., von Houwald, F., Schweizer, R., Kölln, M., Ratert, C., Liesegang, A., 2018. Milk composition of indian rhinoceros (*Rhinoceros unicornis*) and changes over lactation. J. Zoo Wildl. Med. 49 (3), 704–714. https://doi.org/10.1638/2017-0011.1.

Gross, J., Ligges, U., 2015. Nortest: tests for normality. R Pack. Vers. 1 (4).

Guthrie, R.D., 1982. Mammals of the mammoth steppe as paleoenvironmental indicators. Paleoecology of Beringia. Academic Press, pp. 307–326. https://doi.org/10.1016/b978-0-12-355860-2.50030-2.

Guthrie, R.D., 1990. Frozen Fauna of the Mammoth Steppe: the Story of Blue Babe. University of Chicago Press. https://doi.org/10.7208/chicago/9780226159713.001.0001.

Guthrie, R.D., 2001. Origin and causes of the mammoth steppe: a story of cloud cover, woolly mammal tooth pits, buckles, and inside-out Beringia. Quat. Sci. Rev. 20 (1–3), 549–574. https://doi.org/10.1016/s0277-3791(00)00099-8.

Hartman, G., 2011. Are elevated $\delta^{15}N$ values in herbivores in hot and arid environments caused by diet or animal physiology? Funct. Ecol. 25 (1), 122–131. https://doi.org/10.1111/j.1365-2435.2010.01782.x.

Hedges, R.E., Clement, J.G., Thomas, C.D.L., O'Connell, T.C., 2007. Collagen turnover in the adult femoral mid-shaft: modeled from anthropogenic radiocarbon tracer measurements. Am. J. Phys. Anthropol.: Off. Publ. Am. Assoc. Phys. Anthropol. 133 (2), 808–816. https://doi.org/10.1002/ajpa.20598.

Higham, T.F., Jacobi, R.M., Ramsey, C.B., 2006. AMS radiocarbon dating of ancient bone using ultrafiltration. Radiocarbon 48 (2), 179–195. https://doi.org/10.1017/s0033822200066388.

Hobbie, E.A., Högberg, P., 2012. Nitrogen isotopes link mycorrhizal fungi and plants to nitrogen dynamics. New Phytol. 196 (2), 367–382. https://doi.org/10.1111/j.1469-8137.2012.04300.x.

Hobson, K.A., Clark, R.G., 1992. Assessing avian diets using stable isotopes I: turnover of ^{13}C in tissues. Condor 94 (1), 181–188. https://doi.org/10.2307/1368807.

Hoogakker, B.A.A., Smith, R.S., Singarayer, J.S., Marchant, R., Prentice, I.C., Allen, J.R.M., et al., 2016. Terrestrial biosphere changes over the last 120 kyr. Clim. Past 12 (1), 51–73.

Hopkins, D.M., Matthews, J.V., Schweger, C.E. (Eds.), 2013. Paleoecology of Beringia.

Elsevier. https://doi.org/10.1016/c2013-0-10866-5.
Hubberten, H.W., Andreev, A., Astakhov, V.I., Demidov, I., Dowdeswell, J.A., Henriksen, M., et al., 2004. The periglacial climate and environment in northern Eurasia during the Last Glaciation. Quat. Sci. Rev. 23 (11–13), 1333–1357. https://doi.org/10.1016/j.quascirev.2003.12.012.
Iacumin, P., Nikolaev, V., Ramigni, M., 2000. C and N stable isotope measurements on Eurasian fossil mammals, 40 000 to 10 000 years BP: herbivore physiologies and palaeoenvironmental reconstruction. Palaeogeogr. Palaeoclimatol. Palaeoecol. 163 (1–2), 33–47. https://doi.org/10.1016/s0031-0182(00)00141-3.
Jackson, A.L., Inger, R., Parnell, A.C., Bearhop, S., 2011. Comparing isotopic niche widths among and within communities: SIBER–Stable Isotope Bayesian Ellipses in R. J. Anim. Ecol. 80 (3), 595–602. https://doi.org/10.1111/j.1365-2656.2011.01806.x.
Jacobi, R.M., Higham, T.F., Ramsey, C.B., 2006. AMS radiocarbon dating of Middle and Upper Palaeolithic bone in the British Isles: improved reliability using ultrafiltration. J. Quat. Sci.: Publ. Quater. Res. Assoc. 21 (5), 557–573. https://doi.org/10.1002/jqs.1037.
Jacobi, R., Debenham, N., Catt, J., 2007. A collection of early upper palaeolithic artefacts from beedings, near pulborough, west Sussex, and the context of similar finds from the British isles. In: Proceedings of the Prehistoric Society, vol. 73. Cambridge University Press, pp. 229–326. https://doi.org/10.1017/s0079497x00000098.
Jacobi, R.M., Rose, J., MacLeod, A., Higham, T.F., 2009. Revised radiocarbon ages on woolly rhinoceros (*Coelodonta antiquitatis*) from western central Scotland: significance for timing the extinction of woolly rhinoceros in Britain and the onset of the LGM in central Scotland. Quat. Sci. Rev. 28 (25–26), 2551–2556. https://doi.org/10.1016/j.quascirev.2009.08.010.
Jørgensen, T., Haile, J., Möller, P.E.R., Andreev, A., Boessenkool, S., Rasmussen, M., et al., 2012. A comparative study of ancient sedimentary DNA, pollen and macrofossils from permafrost sediments of northern Siberia reveals long-term vegetational stability. Mol. Ecol. 21 (8), 1989–2003. https://doi.org/10.1111/j.1365-294x.2011.05287.x.
Jürgensen, J., Drucker, D.G., Stuart, A.J., Schneider, M., Buuveibaatar, B., Bocherens, H., 2017. Diet and habitat of the saiga antelope during the late Quaternary using stable carbon and nitrogen isotope ratios. Quat. Sci. Rev. 160, 150–161. https://doi.org/10.1016/j.quascirev.2017.01.022.
Kearse, M., Moir, R., Wilson, A., Stones-Havas, S., Cheung, M., Sturrock, S., et al., 2012. Geneious Basic: an integrated and extendable desktop software platform for the organization and analysis of sequence data. Bioinformatics 28 (12), 1647–1649. https://doi.org/10.1093/bioinformatics/bts199.
Kirillova, I.V., Zanina, O.G., Chernova, O.F., Lapteva, E.G., Trofimova, S.S., Lebedev, V.S., et al., 2015a. An ancient bison from the mouth of the Rauchua river (Chukotka, Russia). Quat. Res. 84 (2), 232–245. https://doi.org/10.1016/j.yqres.2015.06.003.
Kirillova, I.V., Tiunov, A.V., Levchenko, V.A., Chernova, O.F., Yudin, V.G., Bertuch, F., Shidlovskiy, F.K., 2015b. On the discovery of a cave lion from the Malyi anyui river (Chukotka, Russia). Quat. Sci. Rev. 117, 135–151. https://doi.org/10.1016/j.quascirev.2015.03.029.
Knott, K.K., Barboza, P.S., Bowyer, R.T., Blake, J.E., 2004. Nutritional development of feeding strategies in arctic ruminants: digestive morphometry of reindeer, *Rangifer tarandus*, and muskoxen, *Ovibos moschatus*. Zoology 107 (4), 315–333. https://doi.org/10.1016/j.zool.2004.07.005.
Kosintsev, P., Mitchell, K.J., Devièse, T., van der Plicht, J., Kuitems, M., Petrova, E., et al., 2019. Evolution and extinction of the giant rhinoceros *Elasmotherium sibiricum* sheds light on late Quaternary megafaunal extinctions. Nat. Ecol. Evol. 3 (1), 31–38. https://doi.org/10.1038/s41559-018-0722-0.
Krajcarz, M., Pacher, M., Krajcarz, M.T., Laughlan, L., Rabeder, G., Sabol, M., et al., 2016. Isotopic variability of cave bears (δ^{15}N, δ^{13}C) across Europe during MIS 3. Quat. Sci. Rev. 131, 51–72. https://doi.org/10.1016/j.quascirev.2015.10.028.
Kuitems, M., van Kolfschoten, T., Tikhonov, A.N., van der Plicht, J., 2019. Woolly mammoth δ^{13}C and δ^{15}N values remained amazingly stable throughout the last~ 50,000 years in north-eastern Siberia. Quat. Int. 500, 120–127. https://doi.org/10.1016/j.quaint.2019.03.001.
Kuc, T., Różański, K., Kotarba, M.J., Goslar, T., Kubiak, H., 2012. Radiocarbon dating of Pleistocene fauna and flora from Starunia, SW Ukraine. Radiocarbon 54 (1), 123–136. https://doi.org/10.1017/s0033822200046798.
Landman, M., Schoeman, D.S., Kerley, G.I., 2013. Shift in black rhinoceros diet in the presence of elephant: evidence for competition? PloS One 8 (7), e69771. https://doi.org/10.1371/journal.pone.0069771.
Lanfear, R., Calcott, B., Ho, S.Y., Guindon, S., 2012. PartitionFinder: combined selection of partitioning schemes and substitution models for phylogenetic analyses. Mol. Biol. Evol. 29 (6), 1695–1701. https://doi.org/10.1093/molbev/mss020.
Leigh, J.W., Bryant, D., 2015. POPART: full-feature software for haplotype network construction. Method. Ecol. Evol. 6 (9), 1110–1116. https://doi.org/10.1111/2041-210x.12410.
Lister, A.M., Stuart, A.J., 2019. The extinction of the giant deer *Megaloceros giganteus* (Blumenbach): new radiocarbon evidence. Quat. Int. 500, 185–203. https://doi.org/10.1016/j.quaint.2019.03.025.
Loog, L., Thalmann, O., Sinding, M.H.S., Schuenemann, V.J., Perri, A., Germonpré, M., et al., 2020. Ancient DNA suggests modern wolves trace their origin to a Late Pleistocene expansion from Beringia. Mol. Ecol. 29 (9), 1596–1610. https://doi.org/10.1111/mec.15329.
Lord, E., Dussex, N., Kierczak, M., Díez-del-Molino, D., Ryder, O.A., Stanton, D.W., et al., 2020. Pre-extinction demographic stability and genomic signatures of adaptation in the woolly rhinoceros. Curr. Biol. 30 (19), 3871–3879. https://doi.org/10.1016/j.cub.2020.07.046.
Lorenzen, E.D., Nogués-Bravo, D., Orlando, L., Weinstock, J., Binladen, J., Marske, K.A., et al., 2011. Species-specific responses of Late Quaternary megafauna to climate and humans. Nature 479 (7373), 359–364. https://doi.org/10.1038/nature10574.
Maechler, M., 2019. Finding groups in data": cluster analysis extended Rousseeuw et. R Pack. Vers. 2, 0.
Massilani, D., Guimaraes, S., Brugal, J.P., Bennett, E.A., Tokarska, M., Arbogast, R.M., et al., 2016. Past climate changes, population dynamics and the origin of Bison in Europe. BMC Biol. 14 (1), 1–17. https://doi.org/10.1101/063032.
McNaughton, S.J., 1979. Grazing as an optimization process: grass-ungulate relationships in the Serengeti. Am. Nat. 113 (5), 691–703. https://doi.org/10.1086/283426.
Müller, S., Tarasov, P.E., Andreev, A., Diekmann, B., 2009. Late glacial to Holocene environments in the present-day coldest region of the northern hemisphere inferred from a pollen record of lake billyakh, Verkhoyansk Mts., NE Siberia. Clim. Past 5, 73–84. https://doi.org/10.5194/cp-5-73-2009.
Olsen, J., Noe-Nygaard, N., Wolfe, B.B., 2010. Mid-to late-Holocene climate variability and anthropogenic impacts: multi-proxy evidence from Lake Bliden, Denmark. J. Paleolimnol. 43 (2), 323–343. https://doi.org/10.1007/s10933-009-9334-7.
Orlando, L., Leonard, J.A., Thenot, A., Laudet, V., Guerin, C., Hänni, C., 2003. Ancient DNA analysis reveals woolly rhino evolutionary relationships. Mol. Phylogenet. Evol. 28 (3), 485–499. https://doi.org/10.1016/s1055-7903(03)00023-x.
Osthoff, G., Hugo, A., de Wit, M., 2008. Milk composition of a free-ranging white rhinoceros (*Ceratotherium simum*) during late lactation. Mamm. Biol. 73 (3), 245–248. https://doi.org/10.1016/j.mambio.2007.06.005.
Owen-Smith, N., 1974. The Social System of the White Rhinoceros. *The Behaviour of Ungulates and its Relation to Management*. IUCN, Morges, pp. 341–351.
Pacher, M., Stuart, A.J., 2009. Extinction chronology and palaeobiology of the cave bear (*Ursus spelaeus*). Boreas 38 (2), 189–206. https://doi.org/10.1111/j.1502-3885.2008.00071.x.
Pečnerová, P., Palkopoulou, E., Wheat, C.W., Skoglund, P., Vartanyan, S., Tikhonov, A., et al., 2017. Mitogenome evolution in the last surviving woolly mammoth population reveals neutral and functional consequences of small population size. Evol. Lett. 1 (6), 292–303. https://doi.org/10.1002/evl3.33.
Pohlert, T., Pohlert, M.T., 2018. Package 'PMCMR'. R package version, 1, 0.
Pradhan, N.M., Wegge, P., Moe, S.R., Shrestha, A.K., 2008. Feeding ecology of two endangered sympatric megaherbivores: asian elephant *Elephas maximus* and greater one-horned rhinoceros *Rhinoceros unicornis* in lowland Nepal. Wildl. Biol. 14 (1), 147–154. https://doi.org/10.2981/0909-6396.
Rabanus-Wallace, M.T., Wooller, M.J., Zazula, G.D., Shute, E., Jahren, A.H., Kosintsev, P., et al., 2017. Megafaunal isotopes reveal role of increased moisture on rangeland during late Pleistocene extinctions. Nat. Ecol. Evol. 1 (5), 1–5. https://doi.org/10.1038/s41559-017-0125.
Raghavan, M., Themudo, G.E., Smith, C.I., Zazula, G., Campos, P.F., 2014. Musk ox (*Ovibos moschatus*) of the mammoth steppe: tracing palaeodietary and palaeoenvironmental changes over the last 50,000 years using carbon and nitrogen isotopic analysis. Quat. Sci. Rev. 102, 192–201. https://doi.org/10.1016/j.quascirev.2014.08.001.
Rambaut, A., Drummond, A.J., Xie, D., Baele, G., Suchard, M.A., 2018. Posterior summarization in Bayesian phylogenetics using Tracer 1.7. Syst. Biol. 67 (5), 901. https://doi.org/10.1093/sysbio/syy032.
Reimer, P.J., Austin, W.E., Bard, E., Bayliss, A., Blackwell, P.G., Ramsey, C.B., et al., 2020. The IntCal20 Northern Hemisphere radiocarbon age calibration curve (0–55 cal kBP). Radiocarbon 62 (4), 725–757. https://doi.org/10.1017/rdc.2020.41.
Rey-Iglesia, A., García-Vázquez, A., Treadaway, E.C., van der Plicht, J., Baryshnikov, G.F., Szpak, P., Bocherens, H., Boeskorov, G.G., Lorenzen, E.D., 2019. Evolutionary history and palaeoecology of brown bear in North-East Siberia re-examined using ancient DNA and stable isotopes from skeletal remains. Sci. Rep. 9 (1), 1–12. https://doi.org/10.1038/s41598-019-40168-7.
Rivals, F., Lister, A.M., 2016. Dietary flexibility and niche partitioning of large herbivores through the Pleistocene of Britain. Quat. Sci. Rev. 146, 116–133. https://doi.org/10.1016/j.quascirev.2016.06.007.
Sher, A.V., 1997. Late-Quaternary extinction of large mammals in northern Eurasia: a new look at the Siberian contribution. Past and Future Rapid Environmental Changes. Springer, Berlin, Heidelberg, pp. 319–339. https://doi.org/10.1007/978-3-642-60599-4_25.
Sher, A.V., Kuzmina, S.A., Kuznetsova, T.V., Sulerzhitsky, L.D., 2005. New insights into the Weichselian environment and climate of the East Siberian Arctic, derived from fossil insects, plants, and mammals. Quat. Sci. Rev. 24 (5–6), 533–569. https://doi.org/10.1016/j.quascirev.2004.09.007.
Stefaniak, K., Stachowicz-Rybka, R., Borówka, R.K., Hrynowiecka, A., Sobczyk, A., Moskal-del Hoyo, M., et al., 2020. Browsers, grazers or mix-feeders? Study of the diet of extinct Pleistocene Eurasian forest rhinoceros *Stephanorhinus kirchbergensis* (Jäger, 1839) and woolly rhinoceros *Coelodonta antiquitatis* (Blumenbach, 1799). Quat. Int. https://doi.org/10.1016/j.quaint.2020.08.039.
Stevens, R.E., Jacobi, R., Street, M., Germonpré, M., Conard, N.J., Münzel, S.C., Hedges, R.E., 2008. Nitrogen isotope analyses of reindeer (*Rangifer tarandus*), 45,000 BP to 9,000 BP: palaeoenvironmental reconstructions. Palaeogeogr. Palaeoclimatol. Palaeoecol. 262 (1–2), 32–45. https://doi.org/10.1016/j.palaeo.2008.01.019.
Stewart, G.R., Turnbull, M.H., Schmidt, S., Erskine, P.D., 1995. ^{13}C natural abundance

in plant communities along a rainfall gradient: a biological integrator of water availability. Funct. Plant Biol. 22 (1), 51–55. https://doi.org/10.1071/PP9950051.
Stuart, A.J., Sulerzhitsky, L.D., Orlova, L.A., Kuzmin, Y.V., Lister, A.M., 2002. The latest woolly mammoths (*Mammuthus primigenius* Blumenbach) in Europe and Asia: a review of the current evidence. Quat. Sci. Rev. 21 (14–15), 1559–1569. https://doi.org/10.1016/s0277-3791(02)00026-4.
Stuart, A.J., Lister, A.M., 2011. Extinction chronology of the cave lion *Panthera spelaea*. Quat. Sci. Rev. 30 (17–18), 2329–2340. https://doi.org/10.1016/j.quascirev.2010.04.023.
Stuart, A.J., Lister, A.M., 2012. Extinction chronology of the woolly rhinoceros *Coelodonta antiquitatis* in the context of late Quaternary megafaunal extinctions in northern Eurasia. Quat. Sci. Rev. 51, 1–17. https://doi.org/10.1016/j.quascirev.2012.06.007.
Studio, R.S.T.R., 2018. Integrated Development Environment. R Studio Inc, Boston, MA.
Stuiver, M., Reimer, P.J., Reimer, R.W., 2021. CALIB 8.2 [WWW program]. at. http://calib.org. (Accessed 29 March 2021).
Szpak, P., Gröcke, D.R., Debruyne, R., MacPhee, R.D.E., Dale Guthrie, R., Froese, D., et al., 2010. Regional differences in bone collagen $\delta^{13}C$ and $\delta^{15}N$ of Pleistocene mammoths: implications for paleoecology of the mammoth steppe. Palaeogeogr. Palaeoclimatol. Palaeoecol. 88–96. https://doi.org/10.1016/j.palaeo.2009.12.009.
van Geel, B., Langeveld, B.W., Mol, D., van der Knaap, P.W., van Leeuwen, J.F., 2019. Pollen and spores from molar folds reflect food choice of late Pleistocene and Early Holocene herbivores in The Netherlands and the adjacent North Sea area. Quat. Sci. Rev. 225, 106030. https://doi.org/10.1016/j.quascirev.2019.106030.
Vartanyan, S.L., Garutt, V.E., Sher, A.V., 1993. Holocene dwarf mammoths from Wrangel island in the Siberian arctic. Nature 362 (6418), 337–340. https://doi.org/10.1038/362337a0.
Wickham, H., 2011. Wiley interdisciplinary reviews: computational statistics. ggplot2, 3 (2), 180–185.
Willerslev, E., Gilbert, M.T.P., Binladen, J., Ho, S.Y., Campos, P.F., Ratan, A., et al., 2009. Analysis of complete mitochondrial genomes from extinct and extant rhinoceroses reveals lack of phylogenetic resolution. BMC Evol. Biol. 9 (1), 95. https://doi.org/10.1186/1471-2148-9-95.
Willerslev, E., Davison, J., Moora, M., Zobel, M., Coissac, E., Edwards, M.E., et al., 2014. Fifty thousand years of Arctic vegetation and megafaunal diet. Nature 506 (7486), 47–51. https://doi.org/10.1038/nature12921.
Wooller, M.J., Zazula, G.D., Edwards, M., Froese, D.G., Boone, R.D., Parker, C., et al., 2007. Stable carbon isotope compositions of Eastern Beringian grasses and sedges: investigating their potential as paleoenvironmental indicators. Arctic Antarct. Alpine Res. 39 (2), 318–331. https://doi.org/10.1657/1523-0430(2007)39[318:scicoe]2.0.co;2.
Yates, J.A.F., Drucker, D.G., Reiter, E., Heumos, S., Welker, F., Münzel, S.C., et al., 2017. Central european woolly mammoth population dynamics: insights from late pleistocene mitochondrial genomes. Sci. Rep. 7 (1), 1–10. https://doi.org/10.1038/s41598-017-17723-1.